Reaction-diffusion dynamics in an oscillatory medium of finite size: Pseudoreflection of waves

A. Rabinovitch,[1] M. Gutman,[1] and I. Aviram[2]
[1]*Physics Department, Ben-Gurion University of the Negev, Beer-Sheva, 84105, Israel*
[2]*35, Shederot Yeelim, Beer-Sheva, 84730, Israel*
(Received 14 October 2002; published 26 March 2003)

Wave propagation in an oscillatory reaction-diffusion, one-dimensional domain of finite size with Dirichlet boundary conditions is analyzed. For sizes below a certain threshold length, the medium cannot sustain wave motion. Above this threshold we find that for a relatively small domain extent, a strong correlation exists between the dynamics of the system and its size. This correlation gradually disappears with increasing domain size. For still larger sizes, we observe an effect of wave *pseudo reflection* near the boundary. It is shown both numerically and analytically that pseudoreflected waves are periodically generated inside the medium by a fast, self-generated ''source'' near the boundary.

DOI: 10.1103/PhysRevE.67.036212 PACS number(s): 05.45.−a, 41.20.Jb

I. INTRODUCTION

Oscillatory (limit cycle, LC) regimes appear in a variety of areas of science and technology, from semiconductor electronics to oscillating chemical reactions and biology (see, e.g., [1,2] and references therein). The most notable example in a living system is the sinus node of the heart [3], which functions as a natural pacemaker for the electric stimulation (action potential) of the organ. At the edges of such a region there usually appears either an excitable domain or a domain devoid of any excitability. Here we concentrate on the LC/excitable interface and consider the question of ''wave reflection'' there. Reflections of waves in a general reaction-diffusion system are rare due to the refractory period of the pulse, which inhibits such occurrences. Noted exceptions to this inhibition are found in only a narrow range of parameter values corresponding to an excitable regime near a subcritical Hopf bifurcation. In this case the collision of a propagating pulse with a spatial nonuniformity results in pulse splitting. The new pulses begin to move in opposite directions, and the backward propagation may be considered as a reflected (or echo) pulse. These reflections occur at the interface between two excitable regions, as well as in an excitable medium with zero-flux boundary, and were analyzed in several papers [4–8]. The question of reflected *autowaves* (waves with refractory edges) in LC media has not been treated so far. The only reflected waves studied in such a medium are of the soliton type in a Ginzburg-Landau system [9,10].

We show in this paper that reflections, or rather *pseudoreflections*, of autowaves are quite abundant in LC domains, and are due to a fast wave source originating near the interface, inside the medium. The term *pseudoreflections* was chosen because the mechanism of this effect is quite different from that of ordinary reflections. In addition, LC domains of short extent sustaining homogeneous bulk oscillations are analyzed, showing that the nature of the wave dynamics strongly depends on the domain size. These phenomena are treated both numerically and analytically. A preliminary result was published elsewhere [11].

II. THE MODEL

A simple one-dimensional (1D) reaction-diffusion system is used here, modeled by two coupled partial differential equations:

$$\frac{\partial v}{\partial t} = v_{xx} + f(v) - w,$$

$$\frac{\partial w}{\partial t} = \varepsilon(v - dw). \tag{1}$$

Here $v(x,t)$ is an *activator*, embodying the *action potential* in neurons or in the heart; $w(x,t)$ is an *inhibitor*, sometimes called the *refractoriness*. The diffusion coefficient D, usually multiplying the term v_{xx}, was omitted from Eq. (1), meaning that all length variables are measured in units of $\sqrt{D}$. In this system, v is the only diffusing variable; ε is a (usually small) parameter measuring the ratio of time constants between activator and inhibitor; d is a parameter. The time t is measured in units of the time constant of the activator v. Note that all parameters and variables are dimensionless. The nonlinear term $f(v)$ is chosen here in two forms. The first is a cubic polynomial in v, corresponding to the FitzHugh-Nagumo (FHN) model [12]:

$$f(v) = v(v-a)(1-v), \tag{2}$$

where a is the *excitability parameter* [13]. Roughly speaking, $a<0$ produces LC behavior, while $a>0$ yields an excitable case. The second form of the nonlinear term $f(v)$ is a piecewise linear version, namely,

$$f(v) = \begin{cases} k_1 v & \text{if } |v| < v_c, \\ -k_2 v + r_c \,\mathrm{sgn}(v) & \text{if } |v| > v_c, \end{cases}$$

$$v_c = r_c k_1/(k_1+k_2), \quad \text{and } r_c = 0.5. \tag{3}$$

The latter version is more amenable to analytical solutions. The region of space considered here is defined to be oscillatory [$a<0$ in Eq. (2)] for $0 \leqslant x \leqslant L$, and excitable ($a>0$) for

$x<0$ and $x>L$. We use Dirichlet boundary conditions at $x=0$ and L (which is equivalent to assuming that a is very large beyond the boundary).

The numerical integration of the differential system (1) was carried out using the unconditionally stable Crank-Nicolson method. The values of time and space intervals, used for all numerical experiments, were Δt and $\Delta x=1$. Control runs carried out with smaller grid values invariably showed the same results. For more details, see Refs. [13,17]. In this paper we use x and i interchangeably ($x=i\Delta x$).

III. MINIMUM SIZE OF A LC MEDIUM

First we follow the method of Keener and Sneyd to obtain the minimal length of a LC region with Dirichlet boundary conditions (BC) which can sustain oscillations. Our description will be brief. For more details see [14].

Consider Eqs. (1) and (2). For a steady state solution we have

$$v_{xx}+f(v_0)-w_0=0,$$

$$w_0=\frac{v_0}{d}, \tag{4}$$

and a similar system for Eqs. (1) and (3). The only solution of Eq. (4) with Dirichlet BC is $v_0=w_0=0$. This is indeed the only solution of Eq. (1) for small values of L. The appearance of oscillating solutions occurs only for larger L values. We thus consider the following perturbation solution near the steady state:

$$v=V(x)e^{\lambda t}, \quad 0<x<L,$$

$$w=W(x)e^{\lambda t}. \tag{5}$$

Using Eq. (5) in Eq. (1) leads to

$$\lambda V=V_{xx}+\left.\frac{\partial f}{\partial v}\right|_0 V-W,$$

$$\lambda W=\varepsilon(V-dW),$$

or

$$V_{xx}+\left.\frac{\partial f}{\partial v}\right|_0 V=\mu V, \tag{6}$$

where

$$\mu=\lambda+\frac{\varepsilon}{\lambda+d\varepsilon} \quad \text{or} \quad \lambda^2+(\varepsilon d-\mu)\lambda+\varepsilon(1-d\mu)=0. \tag{7}$$

A Hopf bifurcation occurs when λ becomes purely imaginary, i.e., when $\mu=d\varepsilon$. As noted in Ref. [14], Eq. (6) is a time-independent Schrödinger equation with the eigenvalue μ. In our case, the cubic $f(v)$ given by Eq. (2) yields $f'|_0=-a$, and Eq. (6) with the Dirichlet BC becomes

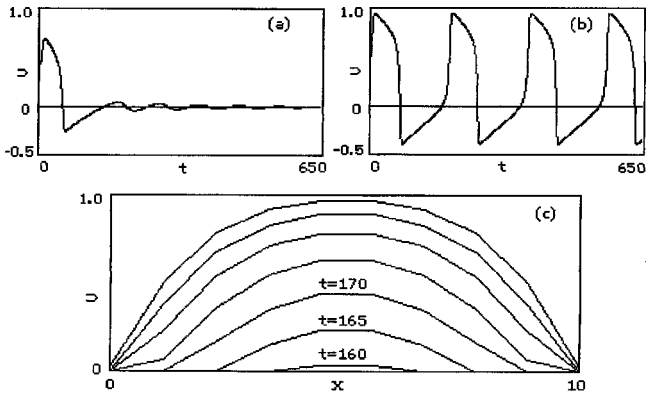

FIG. 1. Dynamics of small LC regions (FHN model with $a=-0.16$, $\varepsilon=0.005$, $d=3$). (a) $L=7$: the initial perturbation vanishes; $v(t)$ is shown at $x=3$. (b) $L=10$: the medium sustains an oscillating response; $v(t)$ is shown at $x=5$. (c) $L=10$: monotonic bulk oscillations of the medium; x profiles of the activator v are shown only during the time interval when v increases from zero to its maximum.

$$V_{xx}=(a+\mu)V, \quad V(0)=V(L)=0. \tag{8}$$

Its solution is $V(x)=A\sin\sqrt{Z}x$, with $Z=-a-d\varepsilon$ and $\sqrt{Z}L=n\pi$. Hence, the minimal length, given by $n=1$, is $L_{\min 1}=\pi/\sqrt{-a-d\varepsilon}$. Alternatively, for the case of a piecewise linear $f(v)$, Eq. (3), we have $f'|_0=0$, $\mu=0$, leading to $L_{\min 2}=\pi/\sqrt{k_1}$.

With the numerical values used here [cubic $f(v)$: $a=-0.16$, $\varepsilon_1=0.005$, $d=3$; piecewise linear $f(v)$: $\varepsilon_2=0.02$, $k_1=0.1$), the two versions of $L_{\min}$ are $L_{\min 1}\sim 8$, and $L_{\min 2}\sim 10$. Numerical simulations show, in fact, that for $L<8$ the only asymptotic solution is $v=w=0$, while oscillating solutions are obtained for $L\geqslant 8$ with the cubic $f(v)$. Figure 1(a) describes the time evolution of an initiating v pulse, launched at time $t=0$, and at site $x=3$ of a medium extending in the range $0\leqslant x\leqslant L=7$. This pulse is a narrow Gaussian in space, and lasts for one Δt in time. An action potential spatial wave is thus generated in the middle of the region and transferred to the boundaries, but the entire spatial wave profile gradually shrinks and eventually disappears after a relatively long period of time (only site $x=3$ is shown). Figure 1(b) depicts the situation when $L=10$, showing the pulse shape as a function of time at point $x=5$. Figure 1(c) depicts the wave amplitude as a function of space at different times. It is seen that the whole medium oscillates in unison (phase locking), a phenomenon well known for LC media. Similar results are obtained for the piecewise linear system.

IV. MONOTONIC BULK OSCILLATIONS

To clarify the influence of the size L ($>L_{\min}$) of the LC medium on the parameters of its oscillations, let us first consider the piecewise linear system with Dirichlet BC. When the medium size slightly exceeds the $L_{\min}$ value, the motion can be described as an *almost in-phase* (monotonic bulk) oscillation. More precisely, the motion can be envisaged by considering the medium points as oscillators having the same

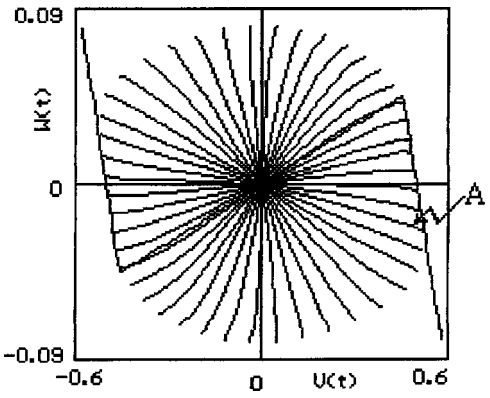

FIG. 2. Phase portraits of *regular isochrones*—lines indicating location of first seven medium points, starting from the Dirichlet BC at a given time (the piecewise linear model with $k_1=0.1$, $k_2=-1$, $\varepsilon=0.02$). Time interval between nearest isochrones is constant, 10 time units, and $L=12$. The deviation from linearity of the isochrone lines suggests out-of-phase oscillations of the medium points.

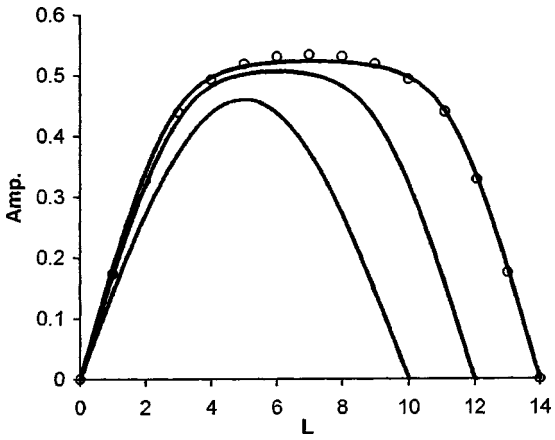

FIG. 3. Analytic solutions corresponding to the piecewise linear model; shown are the maximum values of v (amplitudes) for different medium sizes: $L=10,12,14$, and $\Delta\cong 0,0.03,0.05$ [Eq. (9)], respectively. An increase in L results in the increase of both the amplitude and the period of the monotonic bulk oscillations. The small circles represent exact numerical solutions (maxima) of Eq. (1).

frequency but slightly different phases. To show this we have calculated in the phase plane (v,w) the so-called regular isochrones, i.e., the lines displaying the values of (v,w) at every point of the medium at specific selected times [15]. The slight waviness of the outer edges of the isochrone lines indicates that the motion is not perfectly in phase (see, e.g., Fig. 2). Note that a particular point of an isochrone ray actually represents the values of (v,w) at two spatial points, say, x and $L-x$; this is due to mirror symmetry of the spatial profile.

For comparatively small sizes of the propagation medium (Fig. 2), phase variations are small, and the isochrones appear almost linear. Since isochrone A is the one that includes the absolute maximum of the value of v, we specifically use a linear approximation thereof in order to calculate it analytically. The time derivative is zero along this isochrone, and the following approximate ordinary differential equation can be obtained:

$$0=v_{xx}-\Delta v+\begin{cases}k_1 v & \text{for } |v|<v_c,\\ -k_2 v+r_c\,\mathrm{sgn}(v) & \text{for } |v|>v_c,\end{cases} \tag{9}$$

where $\Delta=(w/v)|_{v_{\max}}$ is the appropriate slope of the isochrone.

Analytic solutions of Eq. (9) for different domain sizes L are shown in Fig. 3. The middle sections of each curve appear to be approximately constant. The larger L, the more extended is this section. Such dynamics is reasonable since increasing L reduces the influence of boundaries on the bulk. It is important to note that this increase of L results in the increase of both the common period T of the oscillating points (see below) and its maximum amplitude $A_{\max}$ (albeit rather slightly) in the middle of the domain. The monotonic dependence of T on L for the case of the piecewise linear model is presented in Fig. 4(a). For this system the change of period can be understood as follows: extended domains induce larger phase-plane trajectories, at least for the central spatial positions. These trajectories are situated along, or very close to, the linear null-cline sections of negative slope for a longer part of the oscillation period. Since the movement there is much slower, the period increases.

We have also calculated a similar dependence of the period T on L for the FHN system [Fig. 4(b)]. The function obtained is slightly nonmonotonic; namely, the values of T first decrease with increasing L, resuming their increase for larger L's (as in the piecewise linear system). This initial ''anomalous'' decrease of T can be explained by comparing phase trajectories corresponding to different values of L (Fig. 5). The oscillations of the less extended medium exhibit slow motions in the vicinity of the unstable fixed point (0,0). A small increase of L results in a displacement of the phase trajectories away from the fixed point and a corresponding decrease of T. Further increase of L brings the motion back into the dominance of the null-clines, and a ''regular'' T vs L dependence is observed.

V. PSEUDOREFLECTED WAVES

A further increase in the length of the LC domain results in the appearance of an interesting effect which we call pseudoreflection at the Dirichlet boundary (Fig. 6). We use this term to emphasize that the mechanism of the creation of these pseudoreflected waves (PRW's) is quite different from the usual reflection mechanism of optical or acoustic waves. The PRW phenomenon for a LC medium was previously observed with different boundary nonuniformities (see [11]). However, the limiting case presented here, i.e., a uniform LC domain with Dirichlet BC, allows us to gain a better understanding based on an analytical description, as well as some important features of the phenomenon.

Along with the usual reversal of propagation direction, the pseudoreflection exhibits the unusual phenomena of decreases of the wavelength, the amplitude, and the period of oscillations. These features, and especially the change of pe-

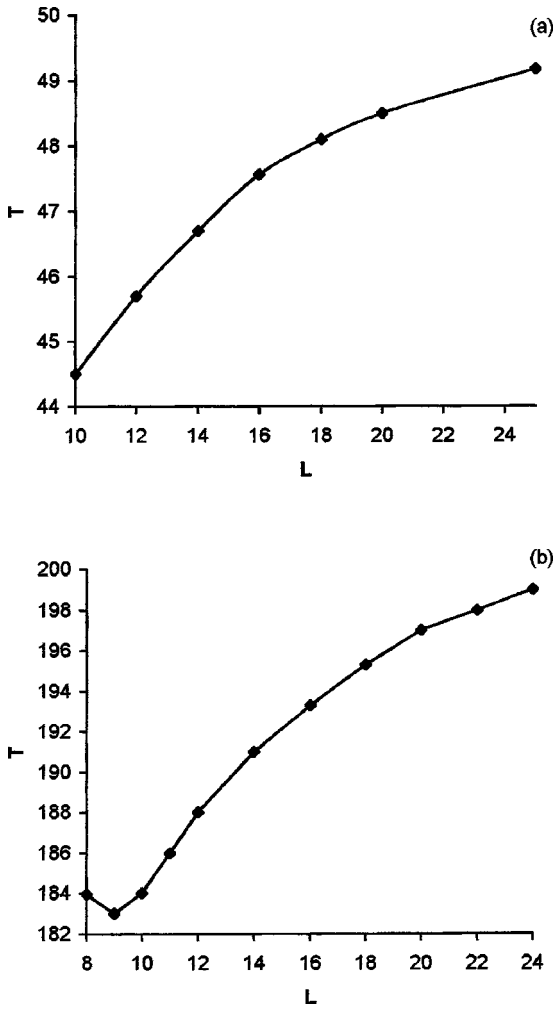

FIG. 4. Variation of the period T of monotonic bulk oscillations as a function of the medium size L. (a) The piecewise linear model with $k_1=0.1$, $k_2=-1$, $\varepsilon=0.02$; (b) FHN model with $a=-0.16$, $\varepsilon=0.005$, $d=3$. Note the nonmonotonic behavior in the latter case.

riod, indicate that other sources of reflected waves have emerged. These higher-frequency sources (drivers) appear close to the Dirichlet boundaries. The piecewise linear model has been utilized to gain a quantitative description of this effect.

Our simulations demonstrate that close to each boundary of the LC medium there exists a spatial transition zone consisting of oscillating points of the medium with monotonically increasing amplitudes away from the boundary. This zone can be looked upon as an array of coupled nonuniform oscillators with different natural frequencies, which synchronize to assume a common frequency, but move out of phase with each other. Increasing the size of the medium causes the phase differences between the points of the transition zone to increase, eventually leading to the generation of propagating waves. Wave generation is well known to appear even in infinite *uniform* LC media, were the wave profile is commonly explained by a symmetry breaking bifurcation [2,16]. In the transition region, however, the oscillators are all different, and one of them eventually assumes the role of the medium ''driver.'' If its precise location were known, one

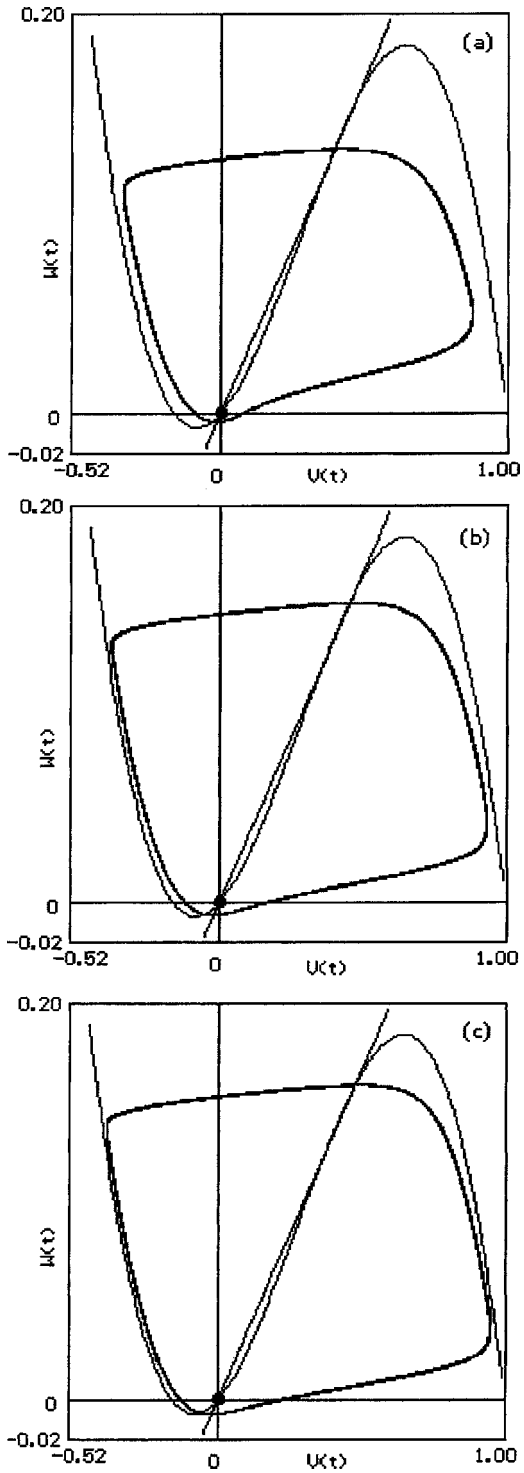

FIG. 5. The FHN model: phase portraits of the oscillations at the centers of spatial domains of different sizes. (a) $L=8$, resulting in $T=184$ time steps. Here the slow motion near the unstable fixed point (●) is responsible for the comparatively large T. (b) $L=9$, resulting in $T=182$ time steps. In spite of a larger limit cycle loop, the value of T decreases because the motion becomes more detached from the fixed point. (c) $L=10$, and T increases back to 184 time steps. The still larger limit cycle loop approaches the null clines (zero-velocity solutions), leading to slower motion in their vicinity.

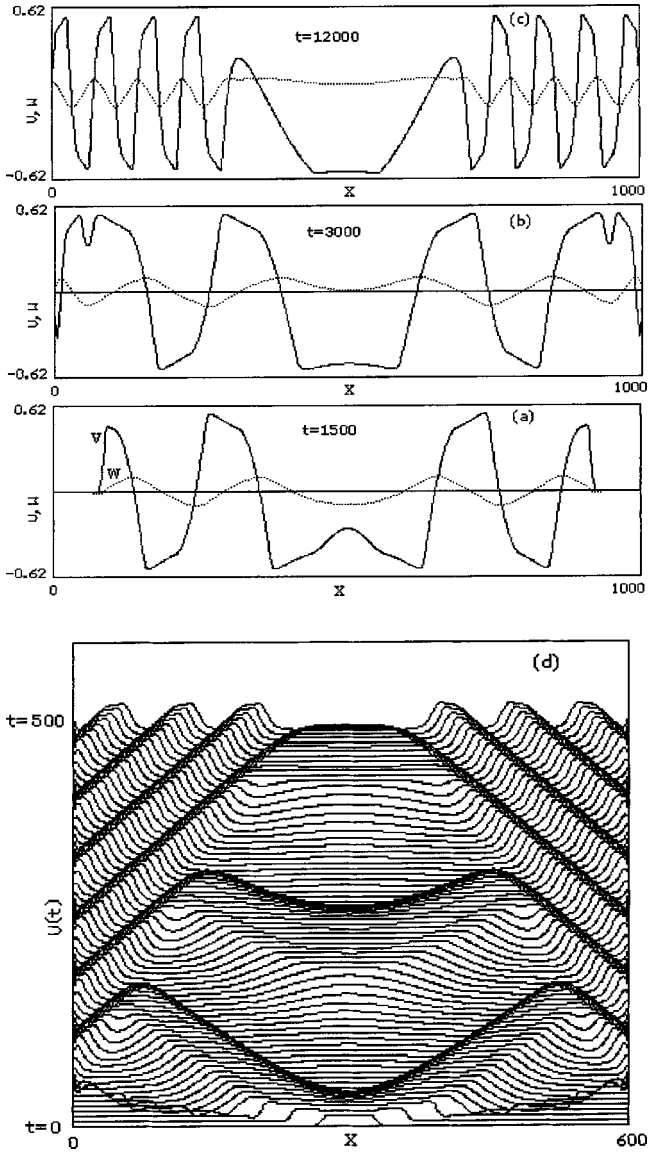

FIG. 6. The pseudoreflected waves in a large-sized LC medium with Dirichlet BC for the piecewise linear model with $k_1=0.1$, $k_2=-1$, $\varepsilon=0.02$. Time increases from bottom to top. (a) Regular waves propagating away from the medium center where a localized initial pulse was launched; (b) these waves drop to zero at the boundaries, but eventually a ''source'' of pseudoreflected waves appears near the boundary, inside the medium, as explained in the text, sending waves in both directions. The inward moving trains are annihilated by collisions with the regular waves. However, because the frequency of the PRWs is higher, the point of annihilation gradually shifts toward the medium center. (c) After a long time only the PRWs are observed. (d) A stroboscopic picture of the propagating and pseudoreflected waves; time difference between the strobes is 10 time units.

would be able to describe the behavior of the entire LC medium by the dynamics of this single oscillator (SO). The ''natural'' frequency of the medium driver should coincide with the common frequency of all other oscillators in the medium, and the location of the driver should determine the direction of the traveling waves.

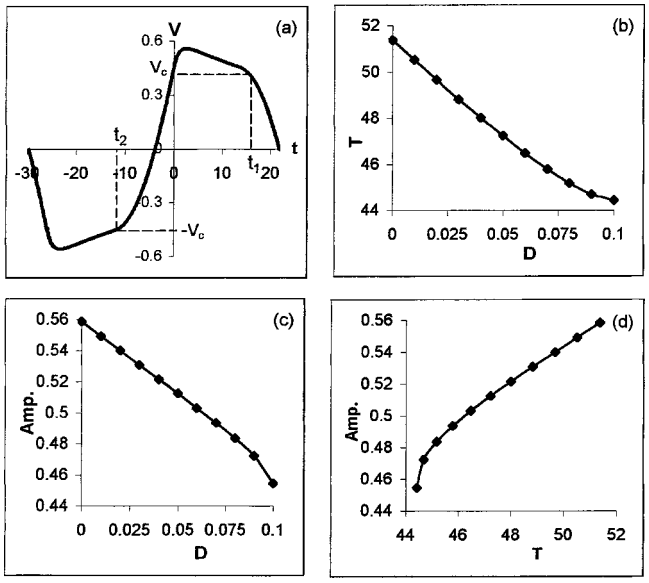

FIG. 7. Dynamics of a single oscillator, made of two uniformly oscillating grid points with Dirichlet BC. Analytical solutions are shown for the piecewise linear model, coinciding with exact numerical results. (a) The wave form of the SO during one period; diffusion coefficient $D=0$. (b) The SO period as a function of D. (c) The SO amplitude as a function of D. (d) The SO period vs its amplitude.

VI. THE INTERNAL (SELF-GENERATED) DRIVER OF PSEUDOREFLECTIONS

In order to simulate SO behavior, a very narrow space domain is examined in this section, where v and w are nonzero only on two grid points (one interval). Since the dependence on the diffusion coefficient D is quite important in this context, it will be explicitly reinstated in the equations. For Dirichlet BC, therefore, we have $v_i=0$, $w_i=0$ at the points $i=0,3$, while at $i=1,2$, $v_i\neq 0$, $w_i\neq 0$. Evidently, since $L_{\min 2}$ is expressed in units of $\sqrt{D}$ in Sec. III, the diffusion constant should be drastically lowered for an oscillatory solution to be possible.

For the simple SO system, an analytical solution is of course possible. To see this we first show that the diffusion term can be converted to a simpler form. Consider the finite difference version of this term with $\Delta x=1$. Since $v_0=0$ and $v_1=v_2$, we have

$$Dv_{xx}|_{i=1}=D(v_2+v_0-2v_1)=-Dv_1. \tag{10}$$

A similar result is obtained for $i=2$. We can therefore replace Dv_{xx} by $-Dv$, or to change k_1 and $-k_2$ of the piecewise linear system by $\Delta k=-D$. The piecewise linear system (with $d=0$) thus becomes

$$\dot{v}=-w+\begin{cases}(k_1-D)v & \text{for } |v|<v_c,\\ (-k_2-D)v+r_c\,\mathrm{sgn}(v) & \text{for } |v|>v_c,\end{cases}$$

$$\dot{w}=\varepsilon v. \tag{11}$$

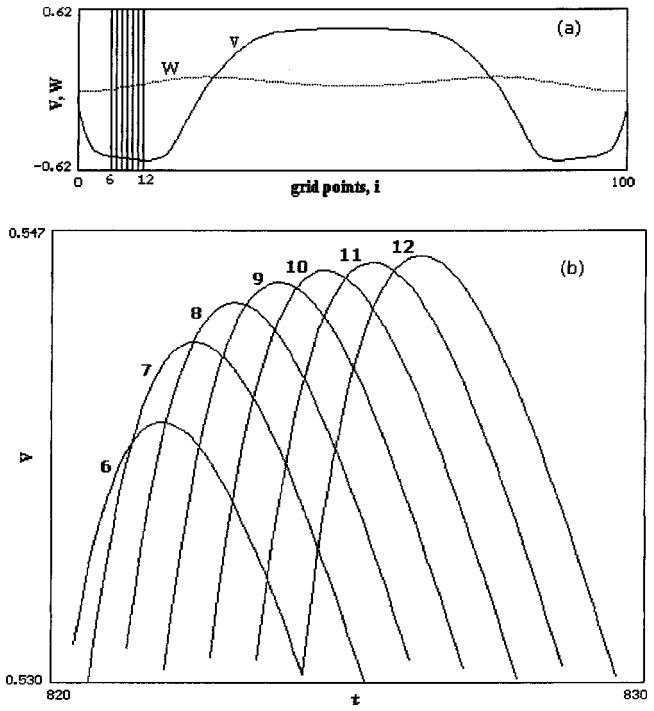

FIG. 8. Determining the position of the PRW ''driver'' in a piecewise linear model with $L=100$. (a) Spatial plot of the PRW at $t=830$ time units; parallel lines near the left boundary ($i=6-12$) indicate seven grid points; (b) local dynamics of these points in the vicinity of their maxima. Point 8 is the first to reach the maximum among its neighbors, thus ''enforcing'' its motion on them.

Taking the derivative of the first equation and using the second, we obtain

$$\ddot{v}=-\varepsilon v+K\dot{v},$$

where

$$K=\begin{cases}(k_1-D) & \text{for } |v|<v_c \quad (\text{denoted by } v_{\mathrm{I}}),\\ (-k_2-D) & \text{for } |v|<v_c \quad (\text{denoted by } v_{\mathrm{II}}).\end{cases} \tag{12}$$

Since in our case $D<k_1$, the solution for $|v|<v_c$ becomes

$$v_{\mathrm{I}}=A_1e^{(k_1-D)t/2}\cos\gamma t+A_2e^{(k_1-D)t/2}\sin\gamma t, \tag{13}$$

where t is measured from the time when $v=v_c$ and $\gamma=\sqrt{\varepsilon-0.25(k_1-D)^2}$. For $|v|>v_c$ the solution is

$$v_{\mathrm{II}}=C_1e^{\lambda_1 t}+C_2e^{\lambda_2 t}, \tag{14}$$

where $\lambda_{1,2}=0.5[-(k_2+D)\pm\sqrt{(k_2+D)^2-4\varepsilon}]$.

The following conditions must be satisfied [Fig. 7(a)]:

$$\text{at } t=0: \quad v_{\mathrm{I}}=v_{\mathrm{II}}=v_c \quad \text{and} \quad \left.\frac{\partial v_{\mathrm{I}}}{\partial t}\right|_0=\left.\frac{\partial v_{\mathrm{II}}}{\partial t}\right|_0;$$

$$\text{at } t=t_1: \quad v_{\mathrm{II}}=v_c \quad \text{and} \quad \left.\frac{\partial v_{\mathrm{I}}}{\partial t}\right|_{t_1}=-\left.\frac{\partial v_{\mathrm{II}}}{\partial t}\right|_{t_2};$$

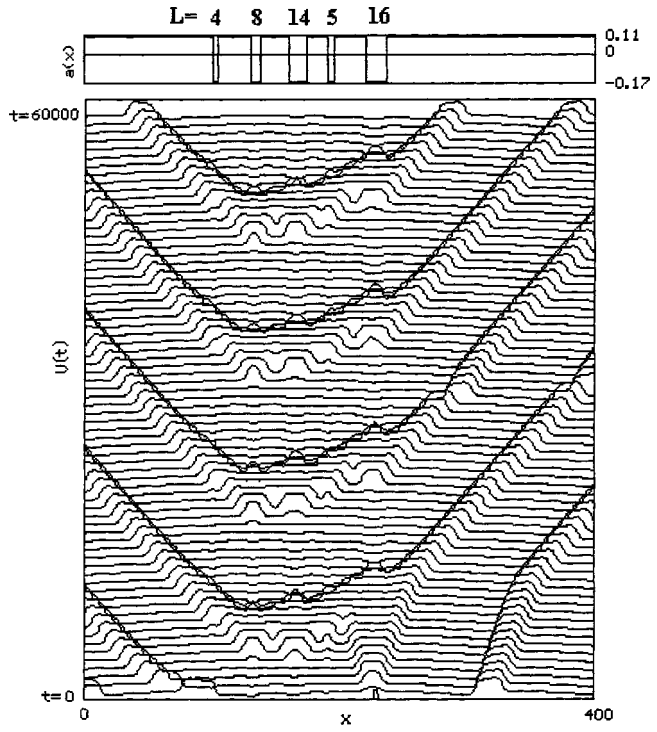

FIG. 9. FHN-based simulations of a ''mosaic'' model: five separate LC sections of different sizes inside a uniform excitable medium. The section with $L=8$ has the highest frequency according to Fig. 4(b), thus becoming the medium driver. After a relatively long transient its natural period of 202 time units eventually dominates the whole medium. Time increases from bottom to top. Note that, unlike the case depicted in Fig. 4(b), here the boundary condition is not of Dirichlet type; hence this period is 202 instead of 184.

$$\text{at } t_2=t_1-T/2: \quad v_{\mathrm{I}}=-v_c.$$

The solution properties are shown in Figs. 7(b) and 7(c). It is clear that both the amplitude and period of oscillations change with D. Note that here $L_{\min 2}=3$ (in units of $\sqrt{D}$) and no nonzero solutions exist for $D\geqslant 0.1$, in agreement with Sec. III. Figure 7(d) shows the functional dependence between the amplitude and the period of the oscillations of v. It is seen that for a SO the higher the frequency (lower T) the lower is the amplitude. Now, in order to drive a whole ''set'' of oscillators, a SO should have both a high amplitude and a high frequency. It is therefore a question of compromise which oscillator of a set will eventually ''take over'' and drive the whole oscillatory region.

In order to check which grid point of the *extended* system becomes the source of the ''reflected'' oscillations (driver), Fig. 8 shows the time dependence of v_i, $i=6-11$, where $v_{i\,\max}>v_c$ ($v_{i\,\max}=v_c$ is situated between $i=3$ and 4) of an oscillatory region of length $L=100$. Since the diffusion current is proportional to v, it is the first grid point where v reaches its maximum relative to both its neighbors, to the left and to the right, that will drive the waves in both directions. In Fig. 8(b) this point appears to be at $i=8$, making this site the ''dominant SO.''

Simulations show that varying the total length L does not change this behavior, namely, the ''sources'' reside at the

same points $i=8$ and $L-8$. The consistency of this result is supported by the following argument: The maximum amplitude (0.543 dimensionless units) of v_8 of the extended system agrees very well with the SO [Fig. 7(d)], having the same period (50 time steps) as that of the waves of Fig. 8.

VII. DISCUSSION

The features of the dynamics of a LC medium of finite length with Dirichlet BC have been discussed. Increasing the medium length leads to the following behavior: (a) for $L < L_{\min}$, no sustained oscillations are present; (b) above $L_{\min}$, a gradual increase of phase mismatch is observed; until (c) the appearance of a propagating train of waves and their pseudoreflections. The mechanism of the PRW generation can be envisaged as due to a fast wave ''source'' or ''driver'' inside the medium, near the boundary. The question of an internal driver of a LC medium is of general importance. Here we have tried to define the properties of such an entity: it is the oscillator that reaches its maximum v value prior to all its neighbors. Thus, via diffusion it can influence the neighboring oscillators on both sides, and become the source (driver) of the pseudoreflected waves.

We wish to point out a number of possible important applications of our findings. The strong dependence of the period of the in-phase oscillations upon the medium size may be of interest for various problems. For example, the problem of an internal pacemaker of the sinus node (SN) arises in the framework of the so-called mosaic model, where the presence of excitable cells inside the sinus node is postulated [18]. A pacemaker is represented by the cluster of oscillating cells, which determines the frequency of the SN in-phase oscillations. Our results support the possibility of such a pacemaker and indicate that this could rather be a section of comparatively small size, although larger than $L_{\min}$ (see Fig. 4), which has the highest oscillation frequency among its neighbors (Fig. 9). It also follows that a relatively small (but still above $L_{\min}$) ectopic source in the heart might be more dangerous than a larger one, because it could oscillate with a higher frequency and lead to serious cardiac arrhythmias. Another important problem of SN oscillations is the possibility of wave propagation there, as opposed to unison (in-phase) oscillations. This type of wave motion was previously discussed in some papers (see, e.g., [19]). These results are consistent with our isochrone-based interpretation showing the development of out-of-phase (wavelike) motion.

The phenomenon of a source of pseudoreflections can, for instance, be applied to the locomotion of a primitive fish (lamprey), which can be modeled as a nonuniform LC medium with an internal driver (the so-called master oscillator). This oscillator is faster than its neighbors, and thus determines the direction of wave propagation in an array of similar surrounding oscillators having lower natural frequencies [20]. Our results indicate that the driver should reside only near either end of a fish of finite length, where Dirichlet-like boundary conditions exist, and should force the lamprey to move in each direction.

[1] R. Kapral and K. Showalter, *Chemical Waves and Patterns* (Kluwer, Dordrecht, 1995).

[2] A. T. Winfree, *The Timing of Biological Clocks* (Scientific American Press, New York, 1987).

[3] L. Glass and M. C. Mackey, *From Clocks to Chaos: The Rhythms of Life* (Princeton University Press, Princeton, NJ, 1988).

[4] V. Petrov, S. K. Scott, and K. Showalter, Philos. Trans. R. Soc. London, Ser. A **347**, 631 (1994).

[5] J. Kosek and M. Marek, Phys. Rev. Lett. **74**, 2134 (1995).

[6] G. B. Ermentrout and J. Rinzel, SIAM (Soc. Ind. Appl. Math.) J. Appl. Math. **56**, 1107 (1996).

[7] O. Aslanidi and O. Mornev, J. Biol. Phys. **25**, 149 (1999).

[8] M. Argentina, P. Coullet, and V. Krinsky, J. Theor. Biol. **205**, 47 (2000).

[9] M. C. Cross and P. C. Hohenberg, Rev. Mod. Phys. **65**, 851 (1993).

[10] M. C. Cross and E. Kuo, Physica D **59**, 90 (1992).

[11] A. Rabinovitch, M. Gutman, and I. Aviram, J. Biol. Phys. **28**, 713 (2002).

[12] R. FitzHugh, Biophys. J. **1**, 445 (1961).

[13] A. Rabinovitch *et al.*, J. Theor. Biol. **196**, 141 (1999).

[14] J. Keener and J. Sneyd, *Mathematical Physiology* (Springer, New York, 1998), pp. 394ff.

[15] A. Rabinovitch and I. Rogatchevskii, Chaos **9**, 880 (1999).

[16] N. Kopell and G. B. Ermentrout, Commun. Pure Appl. Math. **39**, 623 (1986).

[17] A. Rabinovitch, M. Gutman, and I. Aviram, Phys. Rev. Lett. **87**, 084101 (2001).

[18] E. E. Verheijck *et al.*, Circulation **97**, 1623 (1998).

[19] H. Zhang, A. V. Holden, and M. R. Boyett, Nonlinear Anal. Theory, Methods Appl. **30**, 1019 (1997).

[20] T. L. Williams, Neural Comput. **4**, 546 (1992).